Facile Synthesis of Zinc Oxide Nanorods Using a Single-Phase Flow with 3D Printed Device

Pattharaporn Joongpun, Kitikamol Feemuchang, Korakot Onlaor, Thutiyaporn Thiwawong*, and Benchapol Tunhoo

Electronic and Control System for Nanodevices Laboratory, College of Materials Innovation and Technology, King Mongkut's Institute of Technology Ladkrabang, Bangkok, 10520, Thailand.

Received: 7 March 2024, Revised: 15 May 2024, Accepted: 2 June 2024

Abstract

In this work, the single-phase flow chip was applied to synthesize ZnO nanomaterial. The facile process of synthesizing ZnO can be achieved through the printed single-flow chip with the Y-junction pattern. The flow chip was designed and printed with a stereolithography 3d printer. Then, the physical properties of prepared ZnO were performed with an X-ray diffractometer (XRD), Fourier Transform Infrared spectrometer (FTIR), scanning electron microscope (SEM), and UV-visible near-infrared spectrophotometer (UV-Vis-NIR), respectively. It was found that the prepared ZnO exhibited a hexagonal wurtzite structure with the morphologies of ZnO powders, showing the nanorod structure with rod length in micron size. The influence of precursor flow rate on the properties of ZnO nanorods was evaluated. The UV photodetector has been fabricated on a plastic print circuit board with an interdigitated electrode. The optimized sensitivity of the fabricated UV photodetector was investigated.

Keywords: Zinc oxide; Single-phase flow; 3D printed device

1. Introduction

Recently, Zinc oxide (ZnO) nanomaterials are metal oxide in an emerging field of research with the potential to be used in various applications such as optoelectronics, energy, biomedical engineering, and photocatalyst[1]. ZnO has been attracted to comprehensive study due to its unique properties, such as optical and physicochemical properties. At room temperature, ZnO commonly exhibited behaviors of a direct band gap semiconductor with n-type, high thermal stability, and high electron mobility. ZnO nanostructures are candidates for diverse potential applications, such as gas sensors and electrochemical biosensors [2]-[3].

Usually, ZnO nanostructures can be achieved in different dimensional of nanomaterials such as 3D (nanoflowers, porous spheres), 2D (nanosheets, nanofilms), and 1D (nanorods, nanoribbons, nanowires)[4]. The control and modification of ZnO nanostructure are key parameters to prepare ZnO nanomaterials for various applications such as gas sensor devices and photocatalysts [5]-[6]. In those devices, the performance of the fabricated device affects the surface and shape of ZnO. Therefore, the preparation process for producing ZnO nanostructure remained.

Generally, ZnO can be prepared with sol-gel, hydrothermal, vapor phase deposition, co-precipitation, etc. Each process had been offered distinct advantages and limitations. However, the requirement of reproductivity and control of the physical properties of the final ZnO nanostructure is an important key to synthesis techniques. The novel synthesized technique with a flow device on a microfluidic device has been attractive over conventional methods. The advantages of using flow devices in the material synthesis process include real-time spatiotemporal control, good flexibility to integrate with another system, low loss, and low consumption[1], [7]. In the single-phase flow synthesis process, the precursor solutions were fed and reacted in a microflow channel to control reaction parameters and establish the rapid reaction kinetics in the synthesis process. The mass transfer process in the nanomaterial synthesis process can be enhanced by reducing reaction dimensions in the flow channel, which achieves a high synthesis yield in this technique.

This work synthesized the ZnO nanostructure with a single-phase flow process with a flow chip printed with the 3D printer. This technique is low-cost and straightforward for preparing ZnO

Corresponding Author: thutiyaporn.th@kmitl.ac.th

nanostructure. The influence of precursor flow rate on the physical properties of prepared ZnO nanostructure has been evaluated. In addition, the UV photodetector based on synthesized ZnO nanostructure has been fabricated and characterized.

2. Materials and methods

2.1 Design of 3D-printed single-phase flow device

The Y-shape single-phase flow device was applied to synthesize the ZnO nanomaterial. The device was designed with a FreeCAD software program. The single-phase flow chip was printed with a stereolithography 3D printing (Photon Mono 4K) that has a dimension of 35 mm (width) × 76 mm (length) × 2.5 mm (thick). The chip was composed of two input inlets and one output inlet, as shown in the 3D image of the device in Fig. 1 a). The distance between the entrance inlets to the mixing channel, the intersection angle of both input inlets, and the mixing channel length were fixed at 10 mm, 60 degrees, and 125 mm, respectively. The flow channel dimensions were kept at 1 mm x 1 mm in width and height. In addition, the dimensions of the design flow chip are shown in Fig. 1 a) - b).

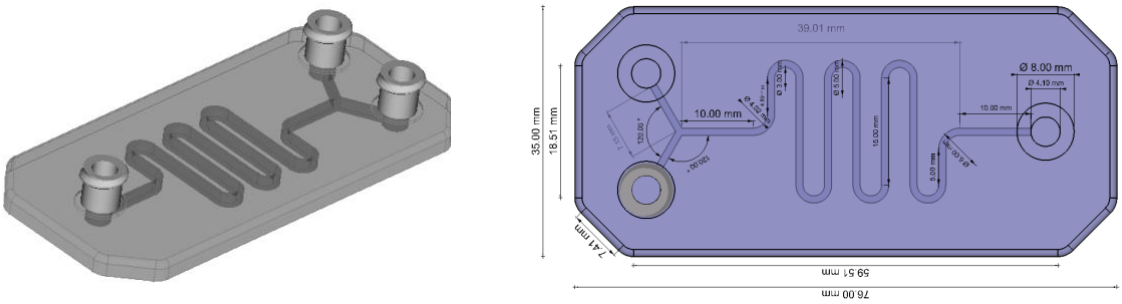

a) b)

Fig. 1. 3D model of Y-shaped single-phase flow device a) Isometric view, and b) Top view

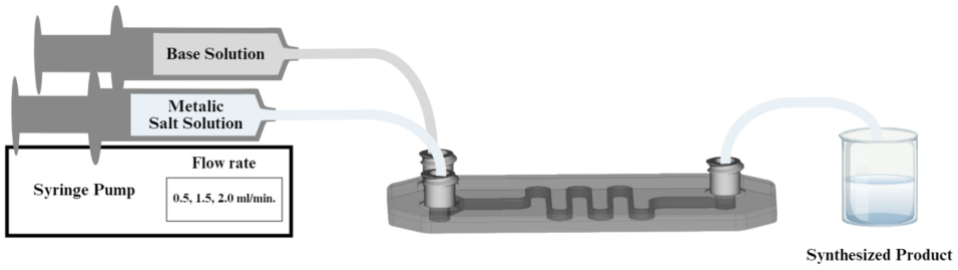

a)

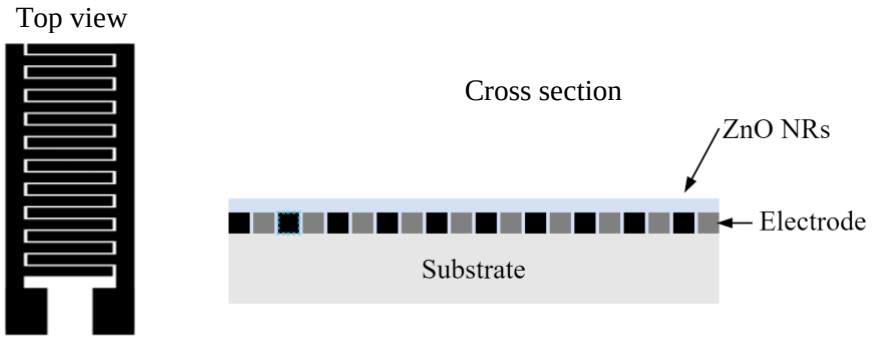

b)

Fig. 2. a) The experimental setup of the single-phase flow for synthesized ZnO nanomaterials, b) The schematic of ZnO photo resistive device

2.2. Synthesis and characterization of ZnO nanomaterials.

Prior, the precursor solutions to prepare ZnO nanomaterial were aqueous solutions of 0.05 M $Zn(NO_3)_2$ and 0.1 M NaOH. The precursor solution was separately contained in each plastic syringe. A syringe pump (NE300) with a 3D printed addition adaptor fed the precursor solutions into the two inlets of the flow device via a PTFE tube with the same flow rate. Fig. 2 a) depicts the experiment setup of the preparation process with a printed Y-shaped single-phase flow device. The flow rates of precursors were controlled at 0.5, 1.0, and 1.5 ml/min. After the precursor solution was fed into the mixing channel, the products of the synthesized reaction were fed out through the outlet channels of the flow chip. Usually, the pH mixing solution is a crucial parameter of prepared ZnO in an aqueous solution. In this work, the pH values of the mixing solution were about 13-14, indicating the stable dispersion of ZnO in the mixing solution [8]. Then, the resulting particles were washed with deionized water until the pH solution was neutral. Finally, the synthesized products were collected and dried in an oven to form solid powders. The physical properties of synthesized ZnO powders were characterized by X-ray diffractometry (XRD, Rigaku SmartLab), Fourier Transform Infrared Spectrometer (FTIR, PerkinElmer Spectrum Two), scanning electron microscope (SEM, Zeiss EVO 15), and UV-VIS-NIR spectrophotometer (HITACHI, UH4150).

2.3 Fabrication of ZnO Photoresistive Device.

The synthesized ZnO nanomaterial was used to prepare a photo-resistive device. The schematic structure of the device is shown in Fig. 2 b). The device substrate was a print circuit board with planar interdigitated electrodes with a spacing distance of 0.25 mm between both electrodes. The synthesized ZnO powders were dispersed in ethylene glycol with a 20 mg/ml concentration. The ZnO films were prepared on the substrate. The electrical characteristics of the prepared photo-resistive device were measured by a precision LCR meter (Keysight E4980AL) with dark and illuminated modes. The optical power of the light source was measured by an optical power meter (Solar Light PMA2100).

3. Result and discussion

The X-ray diffraction spectra of prepared ZnO are shown in Fig. 3. The main XRD peaks were observed at diffraction angles of 31.87 °, 34.48°, 36.32°, 47.62°, 56.65°, 66.54°, and 68.01° that corresponded with the crystal orientation planes of (100), (002), (101), (102), (110), (103), (200), and (112), respectively. The diffraction pattern of all samples exhibited the hexagonal wurtzite crystalline structure of ZnO (JCPDS card No. 36-1451), which confirmed the formation of ZnO with this synthesis process. A dominant diffraction peak was found at 2θ of 36.32°, corresponding with the (101) orientation plane. While the subtle peaks at 2θ of 31.87 ° and 34.48° correspond with (100) and (002) were observed. In addition, the sample prepared with the lowest flow rate showed the lowest XRD intensity and the diffraction peaks were also found to be the other impurities. Typically, the flow of reactants in the flow channel is always laminar due to the microscale flow dimension [1]. With a laminar flow, it is possible to control the reaction in the flow channel from various parameters. Laminar flow will make it possible to control the reaction of substances from various factors. However, the preparation parameters affected the physical properties of the synthesized material.

In addition, the firm peaks at 2θ of 31.87° and 34.48°were assigned as (100) and (002) orientation planes. It indicated the polycrystalline structure of prepared ZnO. The grain size (D) of ZnO powders can be evaluated with Scherrer's equation:

$$D = \frac{K\lambda}{\beta \cos\theta} \quad (1)$$

Where β is full width at half maximum (FWHM), λ is X-ray wavelength, θ is a diffraction angle, and κ is a constant (0.9). The information from a diffraction peak of the (101) plane was used to estimate the crystalline grain size of prepared ZnO. The grain size of synthesized ZnO at flow rates of 0.5, 1.0, and 1.5 ml/min are 18.9, 19.1, and 24.4 nm. It was found that the increase in crystalline structure led to an increase in flow rate according to the formation rate of ZnO particles.

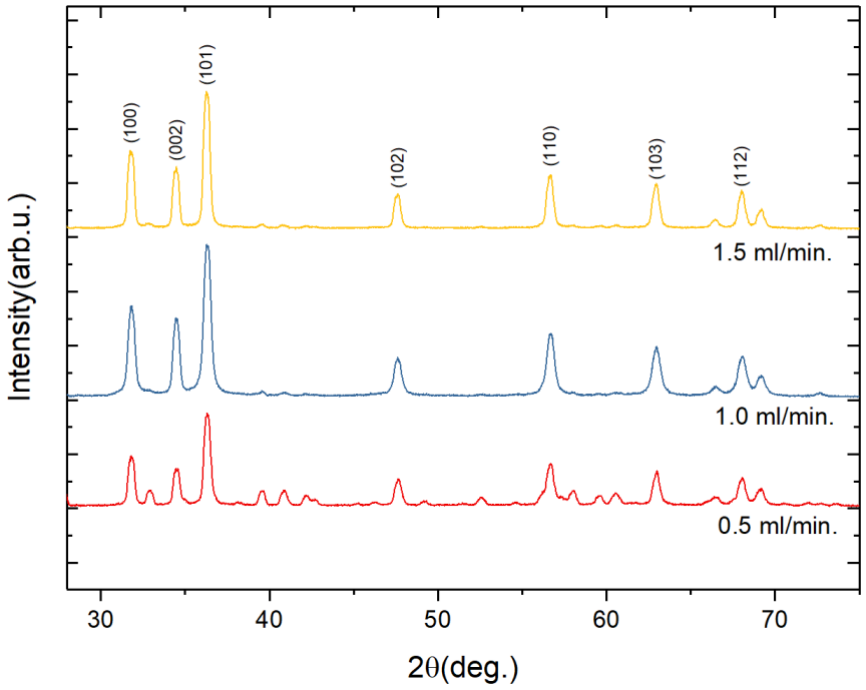

Fig. 3. XRD patterns of ZnO nanorods prepared at various flow rates.

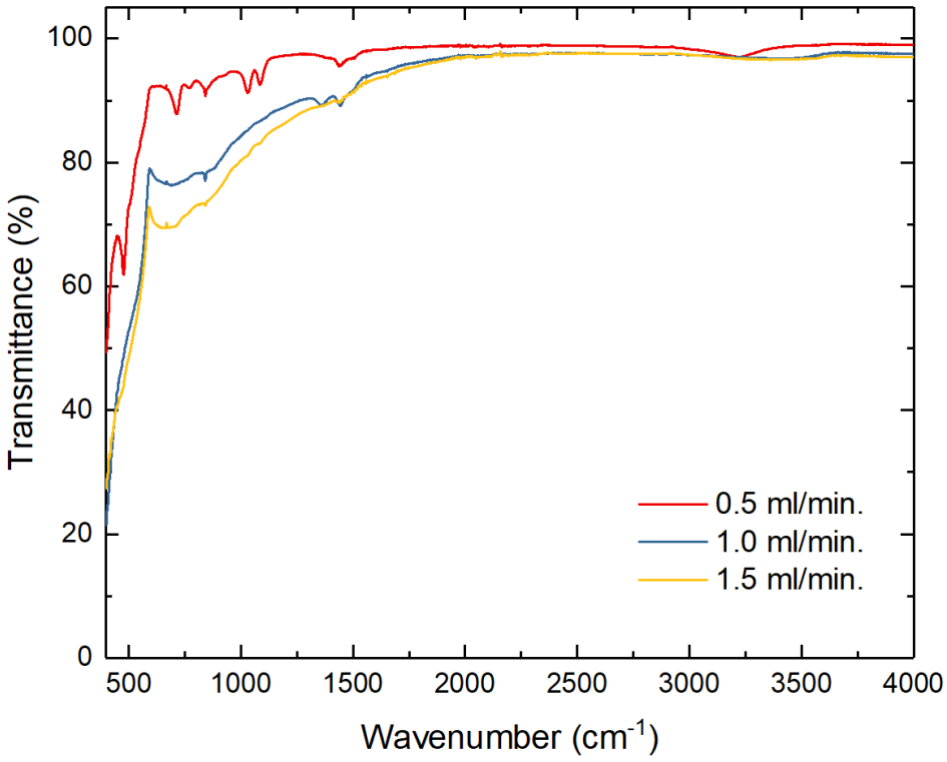

Fig. 4. FTIR spectra of ZnO nanorods prepared at various flow rates

FTIR analysis is a technique to identify the chemical functional characteristics of a material. Fig. 4 shows the FTIR spectra of prepared ZnO powders. The spectra exhibited prominent peaks at 480 cm^{-1}, a characteristic Zn-O bonding peak. Other peaks, such as 715, 838, 1032, and 1089 cm^{-1}, are the impurity phases of organic residue in the material. At the same time, the peak at around 3400 cm^{-1} can be assigned as the result of OH bonding on the surface of ZnO [9]. The prepared ZnO is a highly purified product from the FTR results with this synthesized process.

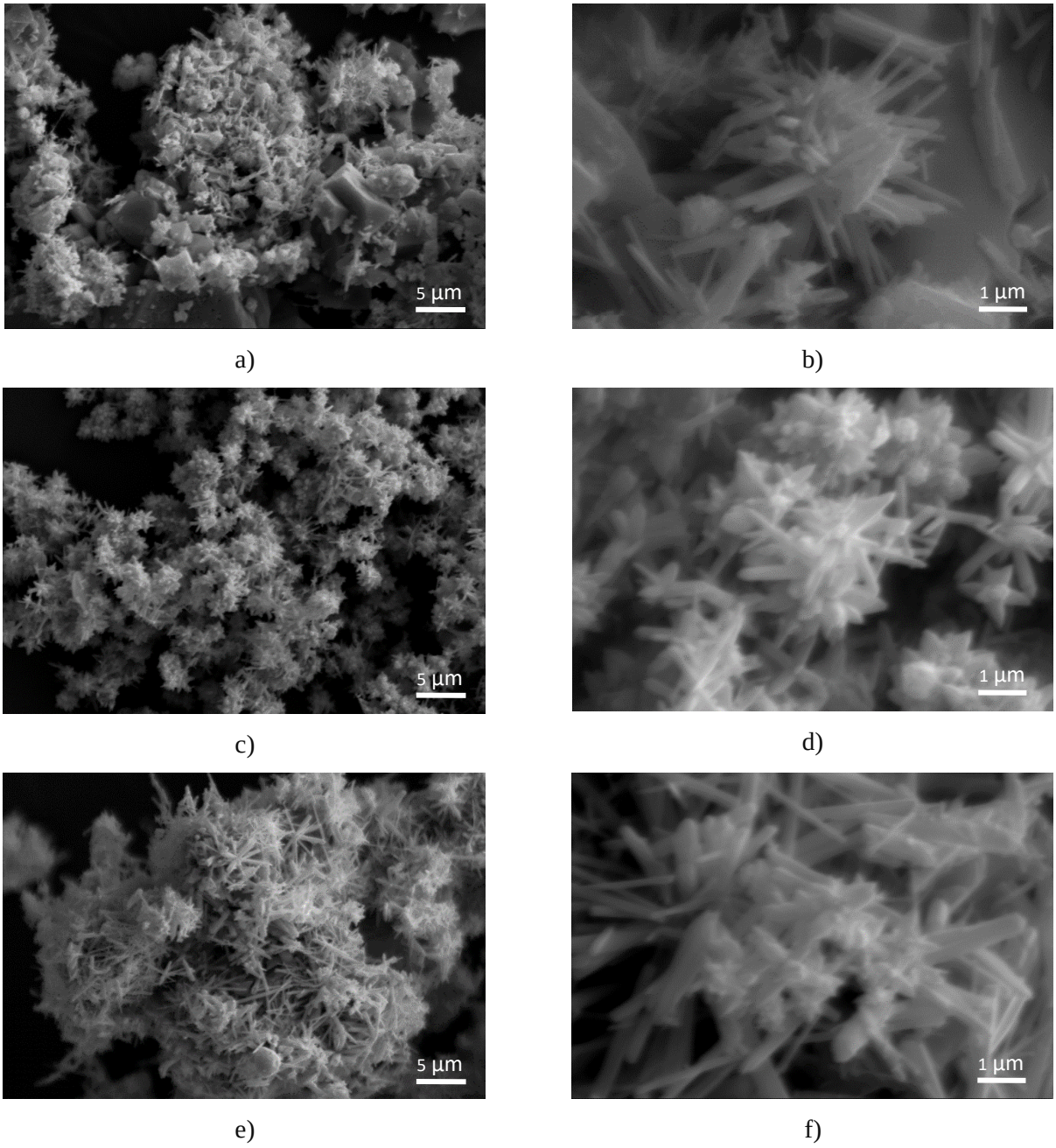

Fig. 5. Morphological images of ZnO nanorods at prepared flow rates of a) - b) 0.5, c) - d) 1.0, e) -f) 1.5 ml/min, and g) Proposed growth directional of ZnO nanorods

The morphologies of prepared ZnO can be achieved by scanning electron microscopy. The prepared ZnO demonstrates the rod-like structure as shown in Fig. 5 a) - f). The average rod diameters are 155.5 ± 62, 211.1 ± 58, and 273.4 ± 77 nm for synthesized flow rates at 0.5, 1.0, and 1.5 ml/min. It was found that the diameter of nanorods increased with increasing the precursor flow rate. It might be due to the influence of nucleation of ZnO during the reaction process in the flow channel. Usually, mixing Zn^{2+} and OH^- ions reacts immediately in the flow channel to achieve a ZnO product. With the high concentration of NaOH base solution, the trend of nuclei of Zn $(OH)_4^{2-}$ has occurred [10]. That is composed of the higher adsorption of Zn $(OH)_4^{2-}$ on the polar positive face in the rich Zn on ZnO [11]. In the other works, the influence of precursor flow rate affected the physical structure of the synthesis product. The effect of flow rate on the spatial dimension of NR ZnO can be observed. The flow rate increased the growth rate due to the higher flow rate reducing the mass transfer boundary layer with increasing ion flux on the surface of prepared nanorod ZnO [12]. Moreover, the high flow rate can maintain the higher concentration of downstream flow precursor. Thus, the diameter of ZnO NRs increased. Therefore, this technique can be applied to prepare ZnO nanorods.

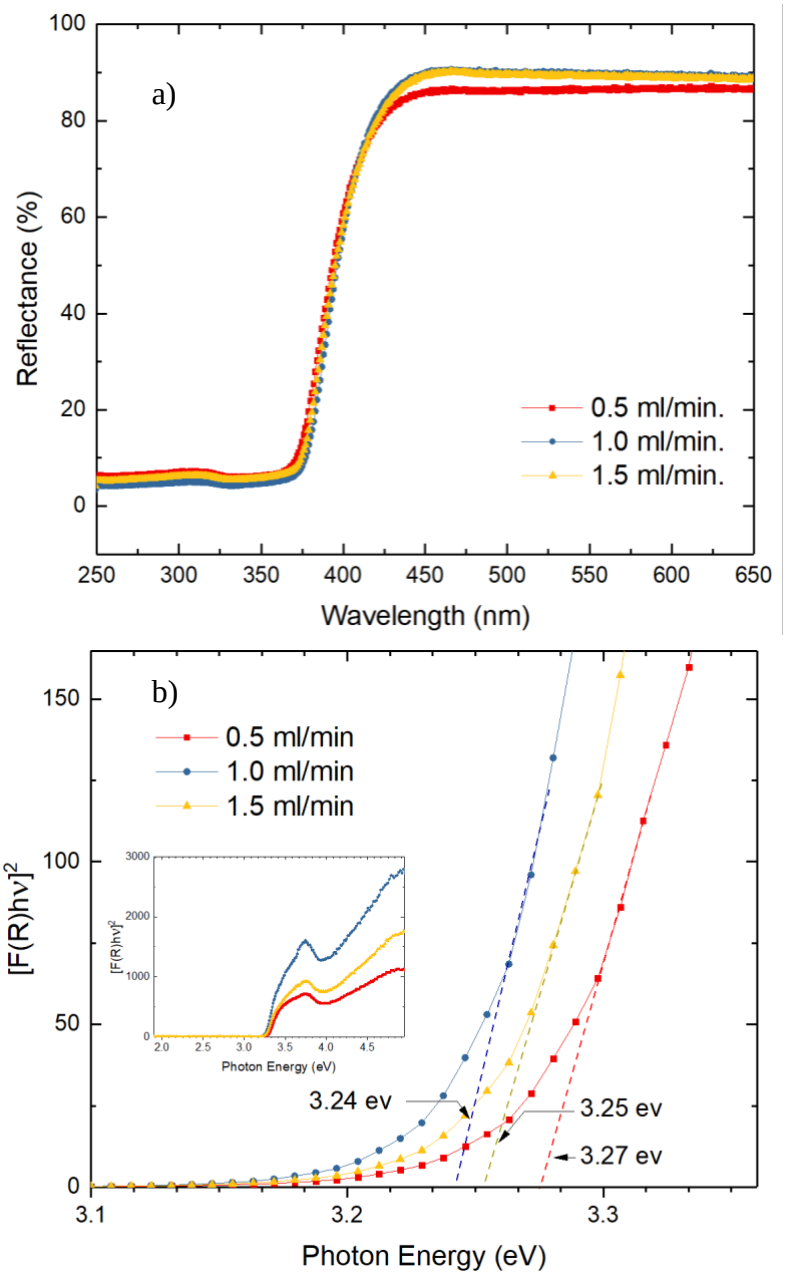

Fig. 6 a) Diffuse reflectance spectra, and b) Kubelka Munk function of ZnO nanorods prepared at various flow rates.

With surface morphologies of the prepared rod-like structure of ZnO, it can be expanded with the growth mechanism described in other works. Zhang et al.[13] had expanded the growth of ZnO nanorods at various annealing temperatures. The HRTEM and SAED images depicted the orientation of crystalline in the (001) growth plane and side planes such as (10-10), (01-10), (1-100), and (-1100). Hu et al. [14] proposed the possibility of ZnO nanorod growth mechanisms in different orientation planes. In the case of the preferred (101) plane, the ZnO orientation might be grown along the c-axis parallel with the pyramid-like structure. For the orientation plane of (101), the crystalline growth parallels the polygon structure. While in the orientation plane of (002), the ZnO nanorod is grown in the vertical c-axis perpendicular, as shown in Fig. 5 g). [15]-[16]

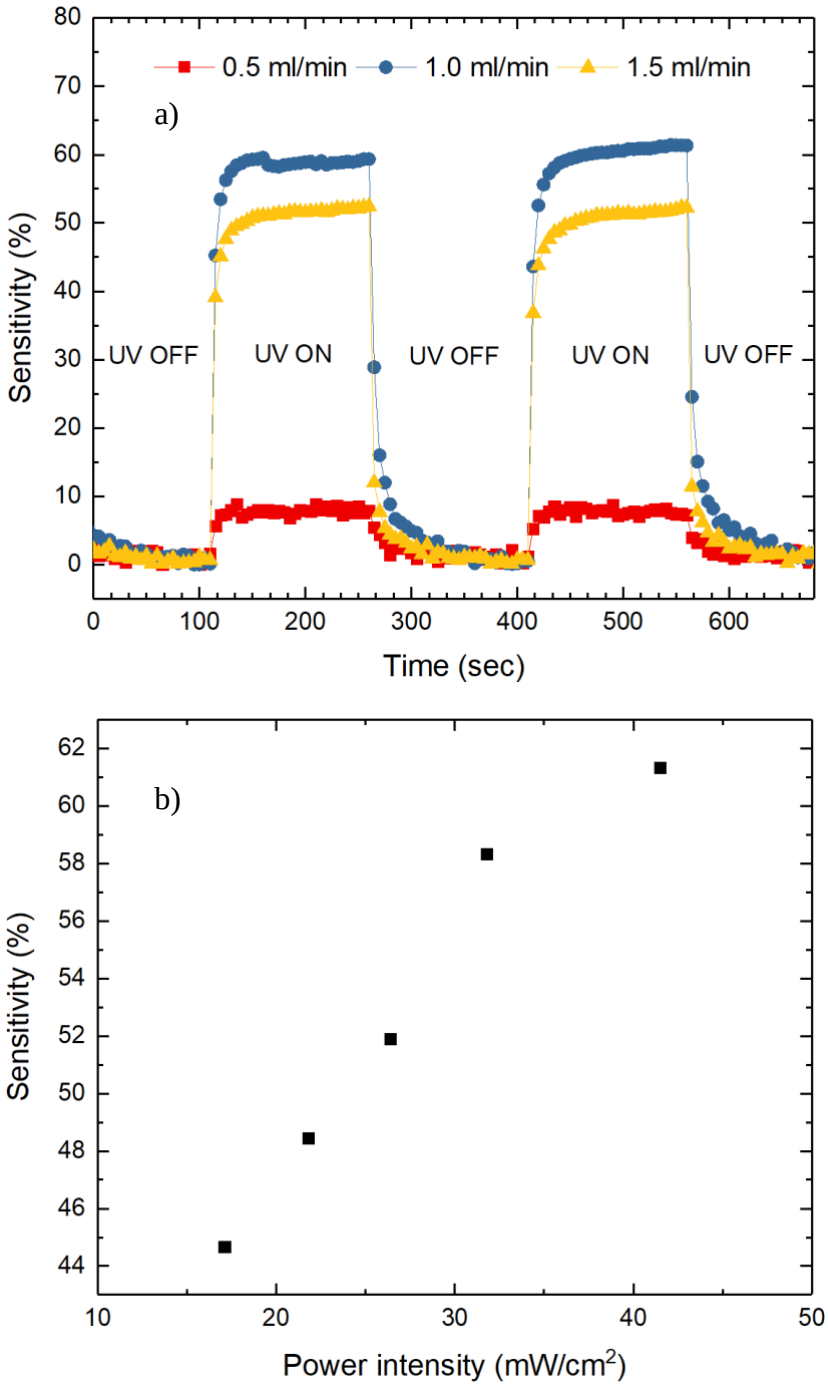

Fig. 7 a) Sensitivity of fabricated ZnO nanorods UV photodetectors, and b) The relation of device sensitivity versus power intensity of UV light source

Fig. 6 depicts the diffuse reflectance spectra of prepared ZnO in a UV-visible region. The reflectance spectra exhibited transition edges around 360 – 400 nm, corresponding to the optical energy band gap of ZnO. The ZnO optical energy band gap was performed using the Kubelka-Munk relation [17] :

$$F(R) = \frac{(1-R)^2}{2R} \quad (2)$$

Where R is the reflectance, the plot of $(F(R) \times h\upsilon)^2$versus photon energy $(h\upsilon)$ is shown in Fig. 6 b). The optical energy band gap of prepared ZnO at flow rates of 0.5, 1.0, and 1.5 ml/min was obtained at 3.27, 3.24, and 3.25 eV, respectively. The variation shifts of optical band gap values might be due to the influence of the crystalline structure of prepared ZnO. The low optical reflection in the UV light region exhibited that prepared ZnO has good behaviors for UV sensing devices.

The synthesized ZnO nanorods were used to prepare a UV photodetector device, as shown in the device schematic in Fig. 2 b). The device was tested under the 390 nm UV lamp illumination with light on and off conditions, as shown in Fig. 7 a). The sensitivity (S) of the photodetector device was estimated from the electrical characteristics at dark and light illumination behaviors. The sensitivity (S) can be calculated following [18]:

$$S(\%) = \frac{(Z_{UV} - Z_{Dark})}{Z_{Dark}} \times 100 \quad (3)$$

Where the S is the sensitivity,$Z_{Dark}$and Z_{UV} are the impedance values of dark and UV illumination conditions. The response time and recovery time were determined from the time of device transition between 10% to 90% and 90% to 10% of output signals. Those values indicated the speed response of the device with the characteristics of ZnO photodetectors are summarized in Table 1. Among ZnO nanorod photodetectors, the device with prepared ZnO at a 1.0 ml/min flow rate exhibited optimized UV sensitivity because its optical band gap can absorb the optical spectrum from the UV lamp. In the case of a decrease in the sensitivity of devices from prepared ZnO at a 1.5 ml/min flow rate, it might be the effect of higher optical energy band gap and more prominent and complex nanoscale rod sizes, which was more light scattering from the device. That was related to the structure properties of those prepared conditions. In addition, the effect of optical power on the sensitivity of the prepared device is shown in Fig. 7(b). It was found that there is a linear relationship between the optical power intensity and the sensitivity of the device.

Moreover, the comparison of photo response characteristics of fabricated ZnO photodetector with other reports is shown in Table 2. The fabricated device can be considered a candidate for a photodetector device with fast response and high sensitivity.

Table 1. Sensing characteristics of fabricated ZnO nanorods photodetectors

Flow rate (ml/min)	Sensitivity (%)	Response Time (s)	Recovery Time (s)
0.5	9.02	13.3	102.5
1.0	61.74	17.1	68.5
1.5	52.38	13.5	32.9

Table 2. Comparison properties of photo response characteristics of various ZnO photodetectors

Materials	Preparation method	Sensitivity	Response Time/ Recovery Time	Ref.
ZnO NRs	Sol-gel	-	3.7 s/ 63.6 s	[19]
ZnO NWs	Vapor-liquid-solid process	12.26	2 s/ 100 s	[20]
ZnO NW/graphene foam	Resistive thermal evaporation	-	9.5 s/38 s	[21]
ZnO films	Successive ionic layers by an adsorption and reaction	-	18 s/24 s	[22]
SnO_2-coated ZnO NWs	Low-temperature method	4.516	1.5 s/25.6 s	[23]
ZnO NRs	Single phase flow	61.74%	17.1 s/68.5 s	This work

4. Conclusion

ZnO nanorods were successfully synthesized without post-thermal treatment annealing. A 3D-printed single-flow chip with different precursor flow rates can achieve the facile process. XRD, FTIR, SEM, and UV-Vis-NIR spectroscopy performed the physical properties of prepared ZnO. The effect of precursor flow rate on the physical properties of prepared ZnO was investigated. It was found that the prepared ZnO exhibited the hexagonal wurtzite structure with nanorod morphologies and rod length on a micro-size scale. The UV photodetector has been fabricated on a plastic print circuit board with the planar interdigitated electrode. The optimized sensitivity of the fabricated UV photodetector was 61.74% at a flow rate of 1 ml/min with linearity of incident optical power.

Acknowledgment

The authors acknowledge the facilities and technical assistance from Nanotechnology and Materials Analytical Instrument Service Unit (NMIS) of College of Materials Innovation and Technology, King Mongkut's Institute of Technology Ladkrabang.

References

[1] Hao, N., Zhang, M., & Zhang, J.X. (2020). Microfluidics for ZnO micro-/nanomaterials development: rational design, controllable synthesis, and on-chip bioapplications. *Biomaterials Science, 8*(7), 1783-1801. DOI:10.1039/c9bm01787a.

[2] Franco, M.A., Conti, P.P., Andre, R.S., & Correa, D.S. (2022). A review on chemiresistive ZnO gas sensors. *Sensors and Actuators Reports, 4*, 100100. DOI:10.1016/j.snr.2022.100100.

[3] Singh, V., & Singh, R. (2022). Simple synthesis of ZnO 3D-hierarchical nanostructures by microfluidics process. *Journal of Materials Science: Materials in Electronics, 33*(18), 14837-46. DOI: 10.1007/s10854-022-08403-6.

[4] Shingange, K., Tshabalala, Z., Dhonge, B.P., Ntwaeaborwa, O.M., Motaung, D.E., & Mhlongo, G.H. (2017). 0D to 3D ZnO nanostructures and their luminescence, magnetic and sensing properties: Influence of pH and annealing. *Materials Research Bulletin, 85*, 52-63. DOI: 10.1016/j.materresbull.2016.09.003.

[5] Kang, Y., Yu, F., Zhang, L., Wang, W., Chen, L., & Li, Y. (2021). Review of ZnO-based nanomaterials in gas sensors. *Solid State Ionics, 360*, 115544. DOI: 10.1016/j.ssi.2020.115544.

[6] Krishnan, R., Shibu, S.N., Poelman, D., Badyal, A.K., Kunti, A.K., Swart, H.C., & Menon, S.G. (2022). Recent advances in microwave synthesis for photoluminescence and photocatalysis. *Materials Today Communications, 32*, 103890. DOI: 10.1016/j.mtcomm.2022.103890.

[7] Gimondi, S., Ferreira, H., Reis, R.L., & Neves, N.M. (2023). Microfluidic devices: a tool for nanoparticle synthesis and performance evaluation. *ACS nano, 17*(15), 14205-14228. DOI: 10.1021/acsnano.3c01117.

[8] Choi, C-H., Su, Y-W., & Chang, C-h. (2013). Effects of fluid flow on the growth and assembly of ZnO nanocrystals in a continuous flow microreactor. *CrystEngComm, 15*(17), 3326-3333. DOI: 10.1039/C3CE26699K.

[9] Anžlovar, A., Orel, Z.C., Kogej, K., & Žigon, M. (2012). Polyol-mediated synthesis of zinc oxide nanorods and nanocomposites with poly (methyl methacrylate). *Journal of Nanomaterials, 31*(1), 31. DOI: 10.1155/2012/760872.

[10] Zhang, H., Yang, D., Ma, X., Ji, Y., Xu, J., & Que, D. (2004). Synthesis of flower-like ZnO nanostructures by an organic-free hydrothermal process. *Nanotechnology, 15*(5), 622. 10.1088/0957-4484/15/5/037

[11] Ahsanulhaq, Q., Kim, S., Kim, J., & Hahn, Y. (2008). Structural properties and growth mechanism of flower-like ZnO structures obtained by simple solution method. *Materials Research Bulletin, 43*(12), 3483-3489. DOI: 10.1016/j.materresbull.2008.01.021.

[12] McPeak, K.M., & Baxter, J.B. (2009). ZnO nanowires grown by chemical bath deposition in a continuous flow microreactor. *Crystal Growth and Design, 9*(10), 4538-4545. DOI:10.1021/cg900551f.

[13] Zhang, X., Qin, J., Xue, Y., Yu, P., Zhang, B., Wang, L., & Liu, R. (2014). Effect of aspect ratio and surface defects on the photocatalytic activity of ZnO nanorods. *Scientific Reports*, *4*(1), 4596. DOI:10.1038/srep04596.

[14] Yue-Hui, H., Yi-Chuan, C., Hai-Jun, X., Hao, G., Wei-Hui, J., Fei, H., & Wang, Y.X. (2010). Texture ZnO thin-films and their application as front electrode in solar cells. *Engineering*, *2*(12), 973-978. DOI:10.4236/eng.2010.212124.

[15] Azmi, Z.H., Mohd Aris, S.N., Abubakar, S., Sagadevan, S., Siburian, R., & Paiman, S. (2022). Effect of seed layer on the growth of zinc oxide nanowires by chemical bath deposition method. *Coatings*, *12*(4), 474. DOI: 10.3390/coatings12040474.

[16] Abdulrahman, A.F., Barzinjy, A.A., Hamad, S.M., Almessiere, M.A. (2021). Impact of radio frequency plasma power on the structure, crystallinity, dislocation density, and the energy band gap of ZnO nanostructure. *ACS Omega*, *6*(47), 31605-31614. DOI:10.1021/acsomega.1c04105.

[17] Alamdari, S., Sasani, G.M., Lee, C., Han, W., Park, H-H., Tafreshi, M.J., Afarideh, H., & Ara, M.H.M. (2020). Preparation and characterization of zinc oxide nanoparticles using leaf extract of Sambucus ebulus. *Applied Sciences*, *10*(10), 3620. DOI:10.3390/app10103620.

[18] Mohammed, F.K., Beh, K.P., Ramizy, A., Ahmed, N.M., Yam, F.K., & Hassan, Z. (2021). Improvement of Porous GaN-Based UV Photodetector with Graphene Cladding. *Applied Sciences*, *11*(22), 10833. DOI:10.3390/app112210833.

[19] Ahn, S.E., Lee, J.S., Kim, H., Kim, S., Kang, B.H., Kim, K.H., & Kim, G.T. (2004). Photoresponse of sol-gel-synthesized ZnO nanorods. *Applied Physics Letters*, *84*(24), 5022-5024. DOI: 10.1063/1.1763633.

[20] Weng, W., Chang, S., Hsu, C., Hsueh, T., & Chang, S. (2009). A lateral ZnO nanowire photodetector prepared on glass substrate. *Journal of The Electrochemical Society*, *157*(2), K30. DOI:10.1149/1.3264650

[21] Boruah, B.D., Mukherjee, A., Sridhar, S., & Misra, A. (2015). Highly dense ZnO nanowires grown on graphene foam for ultraviolet photodetection. *ACS Applied Materials & Interfaces*, *7*(19), 10606-10611. DOI:10.1021/acsami.5b02403.

[22] Shaikh, S.K., Ganbavle, V.V., Inamdar, S.I., & Rajpure, K.Y. (2016). Multifunctional zinc oxide thin films for high-performance UV photodetectors and nitrogen dioxide gas sensors. *RSC Advances*, *6*(31), 25641-25650. DOI:10.1039/C6RA01750A.

[23] Lin, C-C., Chen, Y-W., Chiang, M-C., Lee, C-H., Tung, Y-L., & Chen, S-Y. (2009). Photoconductive Enhancement of Single-Layer Tin Oxide–Coated ZnO Nanowires. *Journal of The Electrochemical Society*, *157*(2), H227. DOI:10.1149/1.3271100.